Proceedings of the 28th IEEE
EMBS Annual International Conference
New York City, USA, Aug 30-Sept 3, 2006

A multi-input modeling approach to quantify hippocampal nonlinear dynamic transformations

Theodoros P. Zanos, Spiros H. Courellis, Robert E. Hampson, Sam A. Deadwyler, Vasilis Z. Marmarelis, Theodore W. Berger

Abstract—**A multi-input modeling approach is introduced to quantify hippocampal neural dynamics. It is based on the Volterra modeling approach extended to multiple inputs. The computed Volterra kernels allow quantitative description of hippocampal transformations and define a predictive model that can produce responses to arbitrary input patterns. Electrophysiological data from several CA3 and CA1 cells in behaving rats were recorded simultaneously using an array of penetrating electrodes. This activity was used to compute kernels up to third order for single and multiple input cases. Representative sets of kernels illustrate the variability of the dynamics of the CA3-CA1 transformations. Our model's predictive accuracy was evaluated using ROC curves.**

I. Introduction

The synaptic circuitry that includes the CA3 and CA1 areas of the hippocampus is believed to be the route that cortically processed information follows to form long term memory [1]. In case of malfunction, due to aging or damage, a cortical neuroprosthetic device provides a reasonable solution to restore the lost functionality. Implementing such neuroprosthetic devices requires quantitative representation of the transformation performed by the malfunctioning area. Nonparametric, data driven, scalable models with predictive capabilities are excellent candidates to represent hippocampal transformations as they do not require explicit knowledge of the underlying mechanisms.

We already presented a proof-of-concept of the restoration of lost cognitive function through a biomimetic device [2], using acute hippocampal slice preparations to acquire data and create a nonparametric model that quantified the CA3-CA1 functional mapping ([2], [3]). It was a single input / single output model, considering only temporal nonlinear dynamics, based on the Volterra modeling approach adapted for point-process input and output signals.

Manuscript received April 3, 2006. This work was supported by the NIH/NIBIB-funded BioMedical Simulations Resource, the DARPA HAND Program and the NSF-funded ERC-BMES.

T. P. Zanos is with the Biomedical Engineering Department, Viterbi School of Engineering, University of Southern California, Los Angeles, CA 90089 USA (213-740-0340; fax: 213-740-0343; e-mail: zanos@usc.edu).

S. H. Courellis, V. Z. Marmarelis and T. W. Berger are with the Biomedical Engineering Department, Viterbi School of Engineering, University of Southern California, Los Angeles, CA 90089 USA (e-mail: shc@usc.edu).

R. E. Hampson and S. A. Deadwyler are with the Department of Physiology and Pharmacology, Wake Forest University, Winston-Salem, NC 27157 USA, (e-mail: hampson@wfubmc.edu)

In this study, we use data from live, behaving rats recorded contemporaneously from several spatially distinct sites at CA3 and CA1, while the rats were performing a memory task. Consequently, the functional relationship between the CA3 and the CA1 hippocampal region has a spatial and a temporal dimension with nonlinear characteristics.

Parametric methods used to model this circuitry (e.g., [4], [5]. [6]) lead to complex, large-scale representations that may not be implementationally friendly for a neuroprosthetic device. Thus, we employed the Volterra modeling approach generalized for multiple inputs. Our effort focused on the computation of Volterra kernels and firing probability functions to achieve maximum predictive accuracy, using natural neural activity recorded in individual CA3 and CA1 neurons during a DNMS (Delayed-NonMatch-to-Sample) task.

II. Methodology

A. Data Collection

A multi-electrode array of penetrating electrodes was used to record the contemporaneous spike activity in the CA3 and CA1 areas ([7], [8]); a conceptual representation of it is shown in Figure 1.

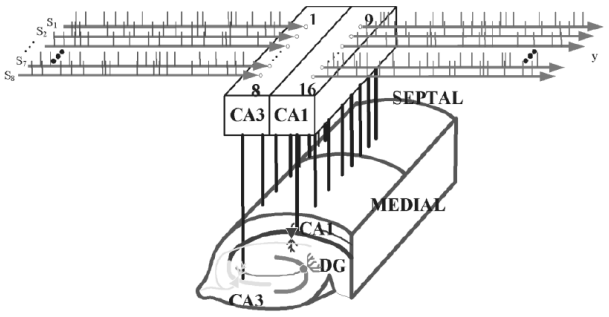

Fig. 1. Conceptual representation of the multi-electrode array recording from the CA3 and CA1 hippocampal regions of the behaving rat.

This array of sixteen electrodes recorded neural activity from multiple cells in the CA3 and the CA1 hippocampal region of the behaving rats, during the DNMS task. The recorded neural activity was in the form of action potentials and was converted to binary spike sequences of variable interspike intervals. The sequence of behavioral events during the DNMS task included a Sample Event (rat hitting

a lever), nose-pokes (for distraction purposes) and a NonMatch Event (rat hitting a lever different from the initial one). Figure 2 illustrates the three different phases during a DNMS trial. Neurons that exhibited low firing rate (<0.2spikes/sec) were excluded as unresponsive and neurons with high firing rate (>6spikes/sec) were excluded, as they were considered to be inter-neurons.

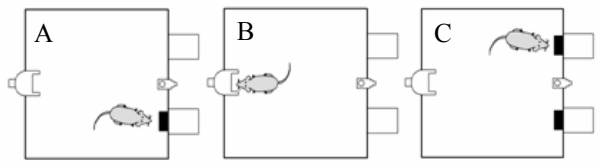

Fig. 2. Illustration of the behavioral tasks the live rat is performing in each trial of the experiment. (A) Left Sample, (B) Delay phase, (C) Right Non Match

B. Mathematical Methods

This class of input / output datasets was used to compute the Volterra kernels of a third order model mathematically expressed as follows:

$$u(n) = k_0 + \sum_{q=1}^{Q}\sum_{m=0}^{M-1} k_{1ps_q}(m)s_q(n-m) + \\ + \sum_{q}\sum_{m_1,m_2} k_{2ps_qs_q}(m_1,m_2)s_q(n-m_1)s_q(n-m_2) + \\ + \sum_{q}\sum_{m_1,m_2,m_3} k_{3ps_qs_qs_q}(m_1,m_2)s_q(n-m_1)s_q(n-m_2)s_q(n-m_3) \quad (1)$$

$$v(n) = f(u) \\ r(n) = TT[v] = \begin{cases} 1 & if\ v > \theta \\ 0 & otherwise \end{cases} \quad (2)$$

where Q is the number of inputs $s_q(n)$, $\{k_0, k_1, k_2, k_3\}$ represent the zero, first, second, and third order Volterra kernels for the corresponding inputs s_q, and $u(n)$ denotes the output of the kernel subsystem. The output of the kernel subsystem $u(n)$ is passed through the firing probability function $F(u)$. The firing probability function associates each value of $u(n)$ with the probability that it will cause a spike in the output. A threshold is applied on this probability, through a triggering threshold function, that provides the binary output $r(n)$. In this model, schematically shown in Figure 3, the effect of interactions among the various inputs is not considered.

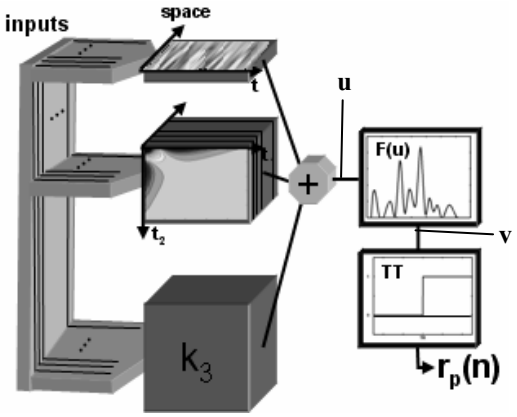

Fig. 3. Schematic diagram of the structure of the proposed multi-input model.

The kernels were computed using the Laguerre expansion method [9]. Employing the orthonormal set of Laguerre functions $\{L_l(m)\}$ to expand the kernels, we obtain:

$$k_1(m) = \sum_{l=0}^{L-1} c^{(1)}_l L_l(m) \\ k_2(m_1,m_2) = \sum_{l_1=0}^{L-1}\sum_{l_2=0}^{L-1} c^{(2)}_{l_1l_2} L_{l_1}(m_1)L_{l_2}(m_2) \quad (3) \\ k_3(m_1,m_2,m_3) = \sum_{l_1=0}^{L-1}\sum_{l_2=0}^{L-1}\sum_{l_3=0}^{L-1} c^{(3)}_{l_1l_2l_3} L_{l_1}(m_1)L_{l_2}(m_2)L_{l_3}(m_3)$$

By using least-squares fitting, we estimate the expansion coefficients and finally compute the kernels. The first order kernel can be interpreted as the effect of each individual input spike on the output. The second order kernel captures the effect of the interaction between pairs of input spikes on the output, while the third order kernel captures the effect of the interaction among triplets of input spikes on the output.

The model's prediction accuracy was evaluated with the use of ROC curves, specifying the optimum performance of our model by the point in the ROC curve that has the smallest distance from the (0, 1) point.

III. Results

Volterra kernels were computed using data recorded during the "non-match" behavioral event. The Volterra kernels were computed using three Laguerre basis functions.

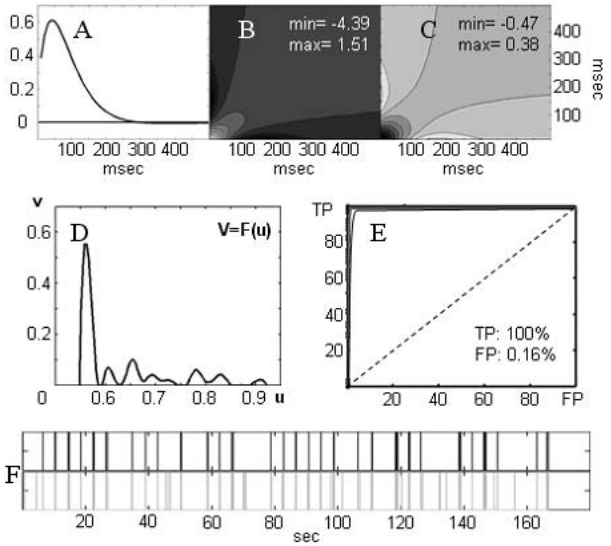

Fig. 4. First (A), second (B) and slice at 50msec of the third (C) order kernels, in the case of one input. Black color corresponds to the minimum value and white to the maximum. Firing probability function (D), ROC curve (E) and a segment of the actual (F-top) and predicted (F-bottom) output.

Several instances of the "non-match" event were considered across a number of different DNMS trials. Each instance of a behavioral event included activity of ±1.5 seconds around the leverpress associated with the event.

First we examined single input / single output relationships between CA3 and CA1 neurons. In this case, Q=1 in the model shown in equation (1). An example is shown in Figure 4, where the components of the model (the first, second, third order Volterra kernels and the probability of firing function) are depicted. The ROC curve and the actual and predicted output of the model are also shown in the same figure. Inspection of the kernels suggests that the first order kernel (Fig. 4A) starts with a facilitatory phase that peaks at about 50msec. The second order kernel (Fig. 4B) presents a faster depressive effect in the beginning and the third order kernel (Fig. 4C) presents a faster facilitatory effect in the beginning. The probability of firing function (Fig. 4D) presents high values around 0.5, making this area of output values the most probable to cause a spike in the output.

Although in some cases activity from a single CA3 cell (input) may be sufficient to predict the activity of a CA1 cell, in other cases it is not. In order to improve prediction, we need to include data from multiple sites. The model computed for a case using two inputs (Q=2) is shown in Figure 5.

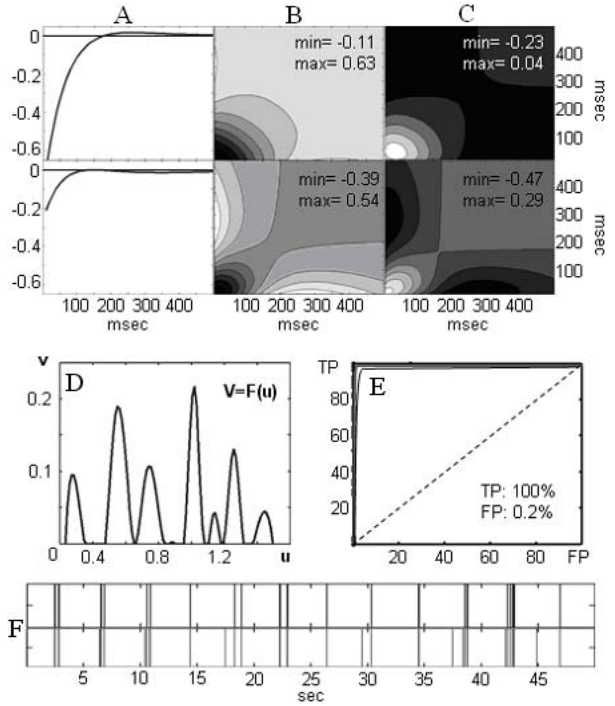

Fig. 5. First (A), second (B) and slice at 50msec of the third (C) order kernels, for each one of the two inputs (top and bottom). Firing probability function (D), ROC curve (E) and a segment of the actual (F-top) and predicted (F-bottom) output show the predictive accuracy of our model.

The first order kernel has a depressive initial phase for both inputs. However, there is a difference in size and duration between the two kernels. The depressive phase of the first order kernel of the first input (Fig. 5A-top) is three times larger and two times slower, since it extends till 200msec. The second order kernels of both inputs present a faster facilitatory effect in the beginning, as shown in Figure 5B. *F(u)* (Fig. 5D) presents multiple peaks at various values of the kernel subsystem output, a fact that exemplifies its importance. Applying a trigger threshold directly on the kernel subsystem output (e.g. threshold=0.1) would cause our model to fire erroneously, in this case at the area around 0.4, 0.85 etc. The model successfully predicts all the spikes, showing that we have improvement in prediction with the incorporation of the second input (Fig. 5F).

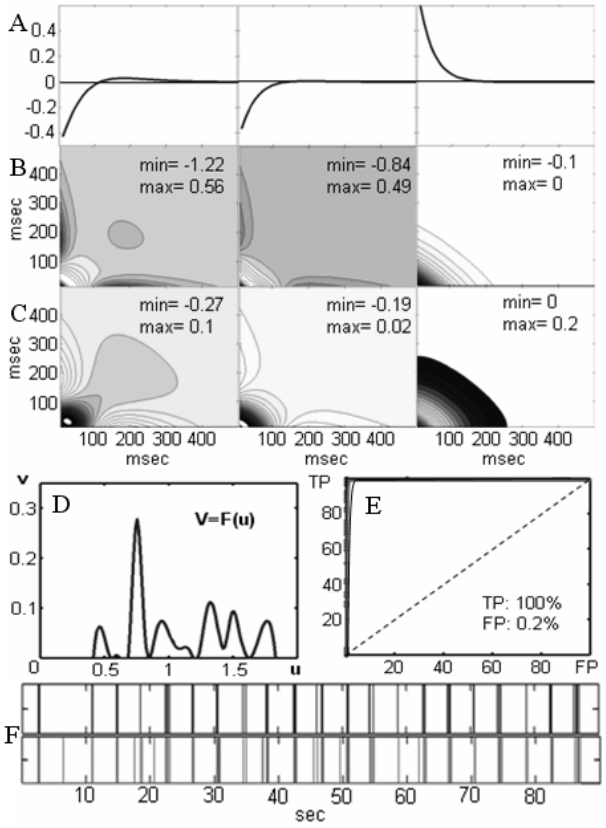

Fig. 6. First (A) second (B) and slice at 50msec of the third (C) order kernels, for each one of the three inputs. Firing probability function (D), ROC curve (E) and a segment of the actual (F-top) and predicted (F-bottom) output show the predictive accuracy of our model.

The value of recruiting more inputs (CA3 cells) to accurately predict the response of a CA1 cell is illustrated by the following example of a three input model (Q=3). The components of the model are shown in Figure 6. In the first two inputs (Fig. 6A-left and 6A-middle), the first order kernels reveal a depressive effect and in the third input (Fig. 6A-right) the first order kernel reveals an excitatory effect. The second order kernels in the case of all inputs (Fig. 6B) present a fast excitatory effect in the beginning. *F(u)* (Fig. 6D) presents a dominant peak around 0.75 and smaller multiple peaks at other values. The model, as shown by the ROC curve (Fig. 6E) and the predicted output (Fig. 6F), succeeds in predicting every spike in the output,

highlighting the positive effect in predictive ability when incorporating three inputs.

Another example of the improvement in prediction when incorporating more than one inputs is depicted in Figure 7. The actual response (Fig. 7C) is compared to model predictions based on a single input (Fig. 7A) and three inputs (Fig. 7B). The single input model fails to predict a number of spikes in the output, while inclusion of three inputs improves our model prediction significantly.

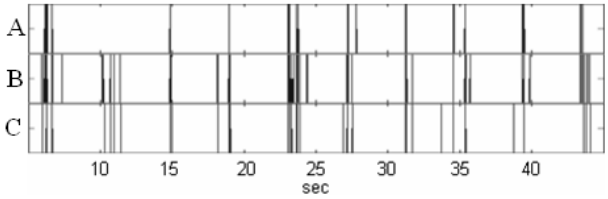

Fig. 7. Improvement in prediction when incorporating more than one inputs. (A) Prediction of the model using one input, (B) three inputs and (C) the actual output.

Following the same thought process, more inputs can be recruited for as long as they increase the model predictive accuracy. An example showing the kernels of a ten input model (Q=10) is depicted in Figure 8. The computed first, second and third order Volterra kernels reveal areas of facilitatory and depressive behavior that vary as functions of space and time.

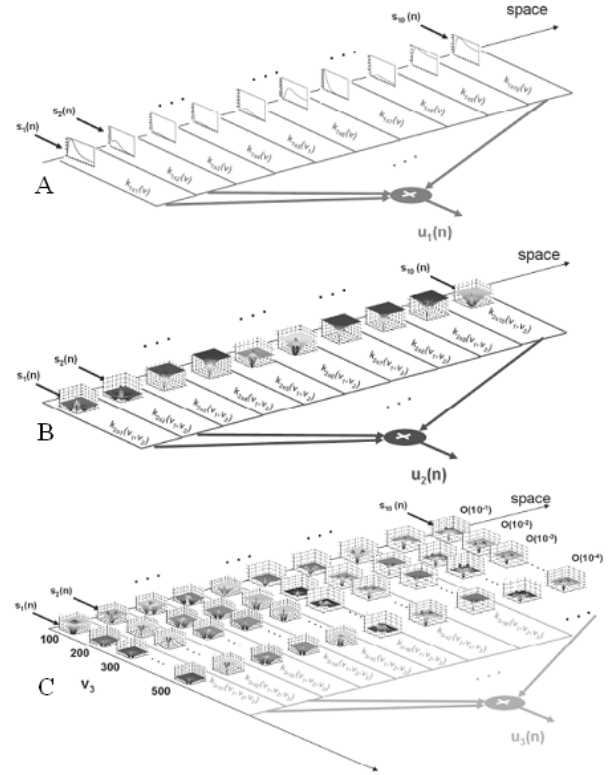

Fig. 8. First (A), second (B) and third (C) order nonlinear kernels for the case of ten inputs.

IV. Discussion

We introduced an extension of the Volterra modeling approach for multiple input hippocampal nonlinear dynamic transformations. We applied the proposed method to model the CA3 to CA1 hippocampal transformations using spike data from behaving rats. Although some times a single CA3 cell (input) was sufficient to predict the response of a CA1 cell, the inclusion of more CA3 cells (inputs) improved the predictive ability of the model.

The presented model does not include cross interactions among the inputs. Incorporating cross interactions and examining the possible improvement of the model's predictive accuracy is the next step. Typically, cross-interactions are present in most neural systems and the hippocampus is not an exception. Including cross-terms in the model that will capture these interactions among the inputs of the system can lead to a higher predictive accuracy, although preliminary results reveal that in some cases their inclusion may not lead to significant improvement.

Our results so far confirm the scalability and the flexibility of the proposed modeling approach. The models derived for the functional mapping from CA3 to CA1 can easily scale up or down to employ the requisite number of inputs, improving the model's prediction accuracy.

References

[1] A. Gruart, M.D. Munoz, J. M. Delgado-Garcia, "Involvement of the CA3-CA1 synapse in the acquisition of associative learning in behaving mice", *Journal of Neuroscience,* vol. 26(4), pp. 1077-1087, Jan 2006

[2] T. W. Berger, A. Ahuja, S. H. Courellis et al, "Restoring lost cognitive function", *IEEE Engineering in Medicine and Biology Magazine*, vol. 24(5), pp. 30–44, Sept.-Oct. 2005.

[3] G. Gholmieh, S. H. Courellis, V. Z. Marmarelis and T.W. Berger, "An efficient method for studying short term plasticity with random impulse train stimuli", *Journal of Neuroscience Methods,* vol. 21(2), pp. 111-127, Dec. 2002.

[4] A. Sargsyan, A. Melkonyan, H. Mikitchian, C. Papatheodoropoulos and G. Kostopoulos, "A computer model of field potential responses for the study of short-term plasticity in hippocampus", *Journal of Neuroscience Methods,* vol. 135(1-2), pp. 175-191, May 2004.

[5] W. B. Levy, "A sequence predicting CA3 is a flexible associator that learns and uses context to solve hippocampal-like tasks", *Hippocampus*, vol 6(6), pp. 579-590, 1996.

[6] E. D. Menschik, S. C. Yen and L. H. Finkel, "Model- and scale-independent performance of a hippocampal CA3 network architecture", *Neurocomputing*, vol. 26-27(1-3), pp. 443-453, 1999

[7] R. E. Hampson, J. D. Shimeral and S. A. Deadwyler, "Keeping on track: Firing of hippocampal neurons during delayed-nonmatch-to-sample performance", *Journal of Neuroscience,* vol. 22(2), RC198 pp. 1-6, 2002

[8] R. E. Hampson, J. D. Shimeral and S. A. Deadwyler, "Distribution of spatial and nonspatial information in dorsal hippocampus", *Nature*, vol. 402(6962), pp. 597-599, Dec. 1999.

[9] V. Z. Marmarelis, *Nonlinear Dynamic Modeling of Physiological Systems.* New York, NY: Wiley, 2004, ch. 2.